EurJOC
European Journal of Organic Chemistry

Full Papers
doi.org/10.1002/ejoc.202100486

Chemistry Europe
European Chemical Societies Publishing

VIP *Very Important Paper*

Special Collection

Mechanistic Study of Domino Processes Involving the Bidentate Lewis Acid Catalyzed Inverse Electron-Demand Diels–Alder Reaction

Marcel A. Strauss[+],[a, b] Daniel Kohrs[+],[a, b] Julia Ruhl,[a, b] and Hermann A. Wegner*[a, b]

The detailed understanding of mechanisms is the basis to design new reactions. Herein, we studied the domino bidentate Lewis acid catalyzed inverse electron-demand Diels–Alder (IEDDA) reaction developed in our laboratory computationally as well as by synthetic experiments, to characterize different pathways. A quinodimethane intermediate was identified as key structure, which is the basis for all subsequent transformations: Elimination to an aromatic naphthalene, rearrangement to a dihydroaminonaphthalene and a photo-induced ring opening. These insights allow to optimize the reaction conditions, such as catalytic utilization of amine, as well as to advance new reactions in the future.

Introduction

The development of new reactions, especially relying on catalysis, is one of the major challenges of today's chemists. Improving efficiency as well as sustainability in all their varieties in accessing any desired molecule is one cornerstone of chemistry. In order to design such new synthetic processes understanding is essential, catapulting mechanistic studies in the center of this endeavor.

One of the most efficient transformations is arguably the Diels–Alder reaction. Highlighted in uncountable total syntheses and beautiful strategies towards molecules, which have been doubted to be existent, there are still new discoveries and applications.[1] In the past decades the inverse electron-demand Diels–Alder (IEDDA) reaction of azines,[2,3] especially tetrazines, has gained increasing attention due to the applicability in click-chemistry in biological environments.[4] While in most cases only azines with three[5] or four nitrogen atoms[6] or electron-withdrawing groups are synthetically useful, we developed in our lab a bidentate Lewis acid catalyzed process allowing the use of 1,2-diazenes in the IEDDA reaction.[7] In our first studies, phthalazines have been converted with suitable dienophiles to the corresponding naphthalenes (Scheme 1, **5**). In the following years, we have been able to take this fundamental reaction to the next level by involving the proposed quinodimethane intermediate **4**[8] in different domino processes accessing highly diverse molecular scaffolds.

Depending on the conditions not only the substituted naphthalene product **5** is obtained, but also a dihydronaphthaleneamine **6**[9] as well as the photo-induced ring-opened (PIRO) product **7** corresponding to a formal insertion of the quinodimethane motif derived from phthalazine **1** into the C=C-bond of the dienophile.[10] Although in all cases a mechanistic proposal has been presented, detailed mechanistic studies have not been conducted. Herein, we investigate the different pathways using computational chemistry providing a full picture of the divergent reactivities.

Results and Discussion

Recently, we established the bidentate Lewis acid catalyzed domino IEDDA/PIRO reaction as an efficient tool to synthesize medium-sized carbocycles (Scheme 2).[11] This transformation

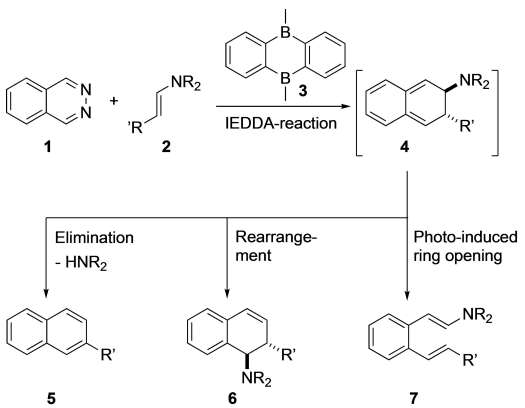

Scheme 1. Divergent reactivity in bidentate Lewis acid catalyzed domino IEDDA reactions.

[a] *M. A. Strauss,[+] D. Kohrs,[+] J. Ruhl, Prof. Dr. H. A. Wegner*
Institute of Organic Chemistry
Justus Liebig University Giessen
Heinrich-Buff-Ring 17, 35392 Giessen, Germany
E-mail: Hermann.a.wegner@org.chemie.uni-giessen.de
https://www.uni-giessen.de/fbz/fb08/Inst/organische-chemie/Wegner
[b] *M. A. Strauss,[+] D. Kohrs,[+] J. Ruhl, Prof. Dr. H. A. Wegner*
Center for Materials Research (LaMa)
Justus Liebig University Giessen
Heinrich-Buff-Ring 16, 35392 Giessen, Germany
[+] *These authors contributed equally to this publication.*

Supporting information for this article is available on the WWW under https://doi.org/10.1002/ejoc.202100486

Part of the "Organocatalysis" Special Collection.

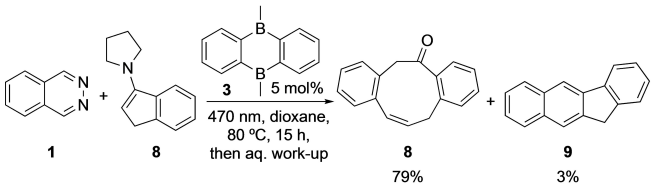

Scheme 2. Bidentate Lewis acid catalyzed domino IEDDA/PIRO reaction of phthalazine (**1**) and enamine **8**.

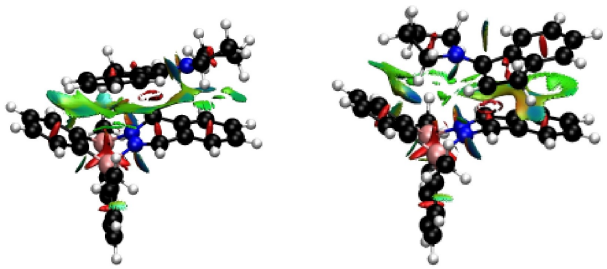

Figure 1. NCI-plot highlighting the attractive London dispersion interactions between the bidentate Lewis acid catalyst and the enamine substrate in the first transition state of the IEDDA-step (left: *exo*, right: *endo*).

has been selected as model reaction in this study. We have chosen DFT computations to shine light on the full mechanistic details of the different domino IEDDA pathways. Geometry optimizations were computed on the PBE0[12] level of theory with a def2-TZVP[13] basis set and the D3-BJ[14] dispersion correction. To account for solvent effects, single point energy (SPE) calculations at the same PBE0-D3BJ level with all optimized structures with the SMD[15] solvent model were carried out. Additional high accuracy single point energy computations on a DLPNO-CCSD(T)/def2-TZVP[16] level were performed using the previously optimized PBE0-D3BJ structures and the Orca 4.2.1[17] software package.

All IEDDA domino processes are initiated by the bidentate catalyzed IEDDA reaction. Therefore, this step will be analyzed first (Scheme 3). The transformation starts with the exergonic coordination of the bidentate Lewis acid catalyst with the diazine-moiety of the phthalazine (**1**). This process lowers the LUMO by 27.1 kcal/mol compared to the parent compound facilitating the critical IEDDA reaction. After this complexation, the dienophile, in this case an enamine, approaches the activated diene. Here, two different pathways can be distinguished, *via* an *endo* and *exo* transition state. The first *endo* transition state **TS-1** (Scheme 3) is preferred by 2.6 kcal/mol compared to the *exo* arrangement, as well as the intermediate **13** (*endo* −10.7 compared to *exo* −9.8 kcal/mol). This observation can be rationalized by attractive London dispersion interactions between the bidentate Lewis acid catalyst and the pyrrolidine-moiety of the enamine (Figure 1). Interestingly, the intermediate **SI-2** (see supporting information), resulting from the *exo*-transition state, is preferred by 2.0 kcal/mol compared to **14**, which can be explained by more favorable π-π-interactions between the phenyl rings of the catalyst and the substrate.

The computed transition states **TS-1** and **TS-2** show, that both bonds are not formed uniformly, but rather in an

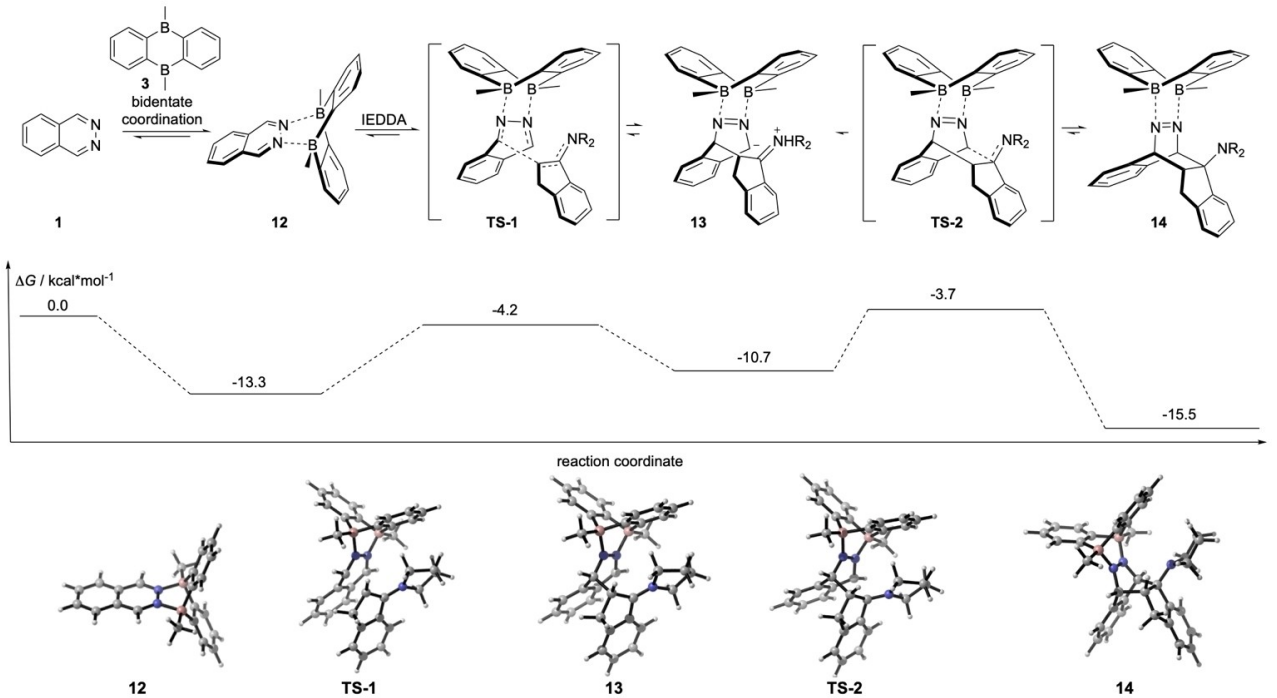

Scheme 3. Initial IEDDA step in the bidentate Lewis acid catalyzed domino reactions.

asynchronous way. The two bonds are formed sequentially, however, with a very low barrier between the first and the second bond forming event. A synchronous transition state, in which both bonds are formed simultaneously, could not be found by computations. Houk and coworkers have shown, that a similar transition state motive is operating in the case of triazenes.[6a,18]

These results suggest, that monodentate Lewis acid catalysts might also be effective. In prior studies, BF_3 and others have been tested to promote the IEDDA reaction of phthalazines without success.[7,9,10] Nevertheless, in this study enamines derived from ketones are employed, which require higher temperatures (110 °C compared to max 60 °C in ref. [9&10]). Interestingly, when BF_3, $B(C_6F_5)_3$ or BPh_3 were employed in all cases the eliminated product **9** was observed, however, with much lower efficiency. With BPh_3 even some of the amine transfer product **21** could be additionally isolated (see supporting information). This observation opens new possibilities to modify the catalyst by an asymmetric substitution pattern at the two boron atoms in the future.

After the IEDDA step, the bidentate Lewis acid should be still coordinated to the dinitrogen-moiety (Scheme 4, **14**). However, the energy difference between the complexed *endo* intermediate **14** and the complexed phthalazine starting material is only 0.3 kcal/mol, allowing a rapid exchange. Although there is the possibility, that the bidentate Lewis acid catalyst **3** is also involved in the N_2-elimination step, this pathway could not be confirmed by computations. The resulting quinodimethane intermediate **16**, after the extrusion of N_2, is key for all domino processes published so far.

In the case of 2-O-substituted furans as dienophiles, a [3,9]-sigmatropic rearrangement was observed.[19] If an additional dienophile is present, the quinodimethane can be trapped *via* a consecutive cycloaddition reaction.[7] In the case of *in-situ* generated enamine dienophiles, different products can be accessed, just by changing the amount of amine, or irradiating the mixture. The latter three processes will be compared computationally in detail. In the case of excess amine, a stepwise concerted reaction path was proposed for the amine transfer reaction, based on computations involving two amine molecules in the transition state (Scheme 5).[9] With equimolar amounts of amine, the elimination was favored, which is in accordance with this proposal. For the elimination, different mechanistic pathways are feasible (Scheme 5). First, a concerted *syn*-elimination would be possible. Second, an E1-type elimination can be proposed, or, third, a bimolecular E2-type reaction involving an additional pyrrolidine as weak base.

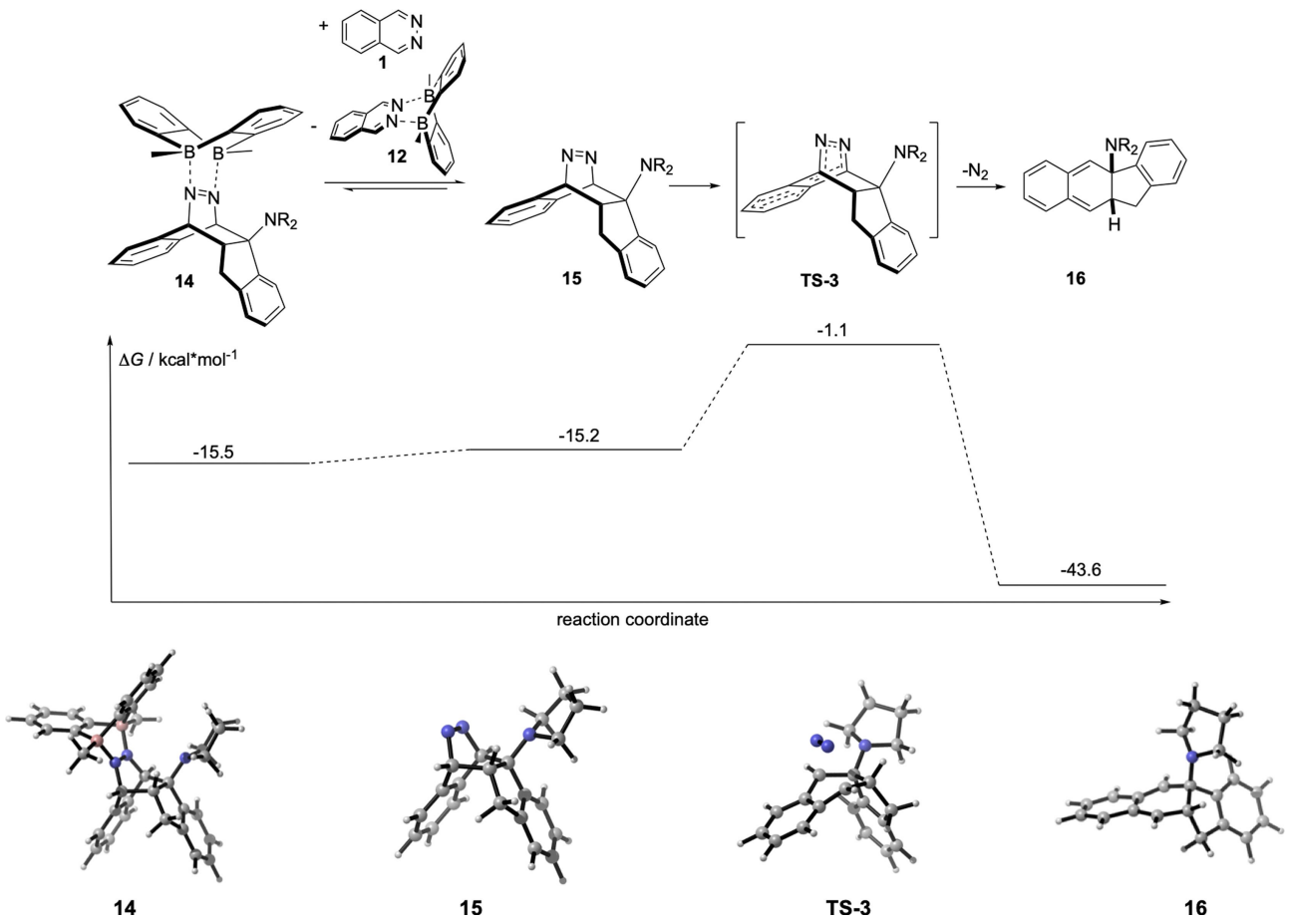

Scheme 4. Elimination of nitrogen to the quinodimethane key intermediate **16**.

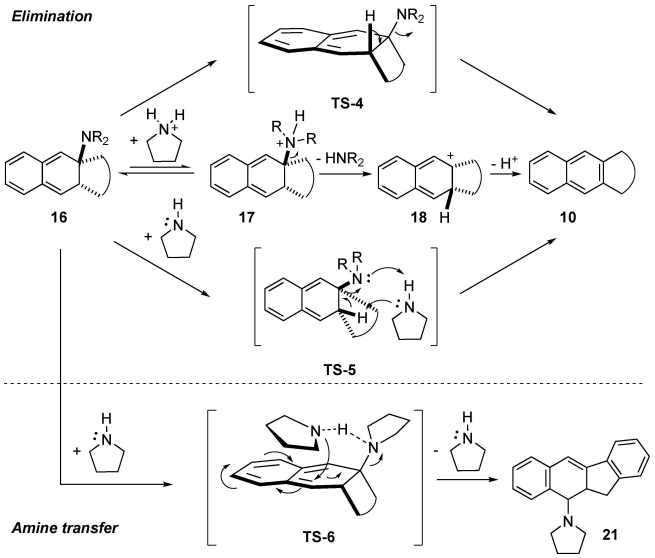

Scheme 5. Mechanistic options for the elimination step of the quinodimethane intermediate **16** to the aromatic product **10** or the amine transfer product **21**.

To support these proposals with experimental data, the model reaction has been conducted with various amounts of amine. No rearranged product was observed with substoichiometric amounts of amine in the presence of molecular sieves, opening the option to conduct the reaction with catalytic amounts of amine (Table 1, entry 1&2). Interestingly, without molecular sieves, even with only 0.5 equiv. of pyrrolidine (**20**), 11% of the rearranged product **21** were isolated. With excess of amine, the eliminated product **10** was formed nearly quantitatively after 4 d of reaction (Table 1, entry 6). However, if the reaction was stopped already after 1 d, in all cases the eliminated product **10** was the main outcome with small amounts of the rearranged product **21**, which is in contrast to our previous findings.[9] Unfortunately, the reaction cannot be conducted at lower temperatures as these temperatures are required for the less reactive ketone. Therefore, the same study has been done for the 3-methylbutanal reaction at 110 °C with 0.5, 1.0 and 2.0 equiv. pyrrolidine (**20**) (see supporting information for details). At this elevated temperature, only elimination product was observed for substoichiometric amounts of amine. With increasing amounts of amine, the ratio of rearranged/eliminated product increased. These findings open additional questions: Does the rearrangement occur in any case, and over time the eliminated product is formed due to the highest thermodynamic stability? Is there a difference between the aliphatic enamine and the here employed aromatic dienophile derived from **19**?

Table 1. Screening of the effect of different amounts of amine in the bidentate Lewis acid catalyzed IEDDA reaction [phthalazine (**1**, 1.00 equiv.), 1-indanone (**19**, 1.00 equiv.) and **3** (5.0 mol%)].

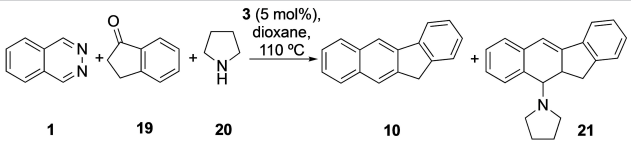

1 19 20 10 21

Entry	Equiv. pyrrolidine (**20**)	Time [d]	Yield **10** [%]	Yield **21** [%]
1[a]	0.2	4	78	–[b]
2[a]	0.5	4	84	–[c]
3[a]	1.0	4	92	5
4[a]	2.0	4	97	–
5	0.5	4	87	11
6	2.0	4	98	–
7	1.0	1	81	16
8	2.0	1	83	15

[a] Molecular sieve (3 Å) was added. [b] 18% of ketone **19** were re-isolated. [c] 14% of ketone **19** were re-isolated.

Hence, all possible elimination pathways (Scheme 5) have been subjected to computational evaluation with 1-indanone (**19**), as well as 3-methylbutanal as an aliphatic example, employed in our earlier study. Interestingly, the concerted *syn*-elimination from the quinodimethane intermediate **16** requires, according to our computations, the highest activation barrier (38.8 kcal/mol). The bimolecular proposal requires 31.7 kcal/mol, which renders also this pathway rather unlikely. The most reasonable mechanism proceeds *via* an E1-type mechanism, though. It is expected, that due to the presence of small amounts of water, the amine will be partially protonated. In the equilibrium between the protonated pyrrolidine and the protonated quinodimethane intermediate **17** the latter is favored by 4.2 kcal/mol. The formation of the following carbocation **18** only requires 15.1 kcal/mol, which ultimately proceeds to the aromatic elimination product **10** in a highly exergonic step. In order to gain an insight into the different reactivities, leading to an amine transfer or an eliminated species, a population analysis was conducted. With this, the charge distribution across the contributing atoms can be quantified. For this purpose, the cations **18** and **22** were compared to a reference system (for details see supporting information). In both cases, the positive charge is stabilized by distribution over the whole π-system. Nevertheless, higher charge densities can be located at specific carbon atoms. The benzyl-annelated naphthyl cation **18** (Figure 2, right) reveals high cationic character at the carbon center, prior connected to the leaving group (charge of +0.231). A further stabilization occurs within the expanded conjugated alkene system, from which one position, leading to a benzylic cation as a resonance structure, is the most favored one (+0.193). Both carbon centers with the highest positive charge profit also from C–H hyperconjugation with the central sp^3-center. The higher extent in partial positive charge (+0.231 *vs.* +0.193) can be rationalized by the substitution pattern (tertiary *vs.* secondary carbon center). In contrast, the *i*-Pr-naphthyl cation **22** shows the reversed charge distribution between the two discussed carbon centers (+0.248 in benzylic position; +0.203 at the former amine-bound carbon). In both cases, one remaining proton carries ~ +0.1 charge. This observation can be explained by an increased acidity, as its deprotonation would give substituted naphthalene derivatives with two aromatic rings as a strong driving force.

NICS(0) values,[20] in combination with the evaluation of bond length alternation (BLA), were consulted in order to

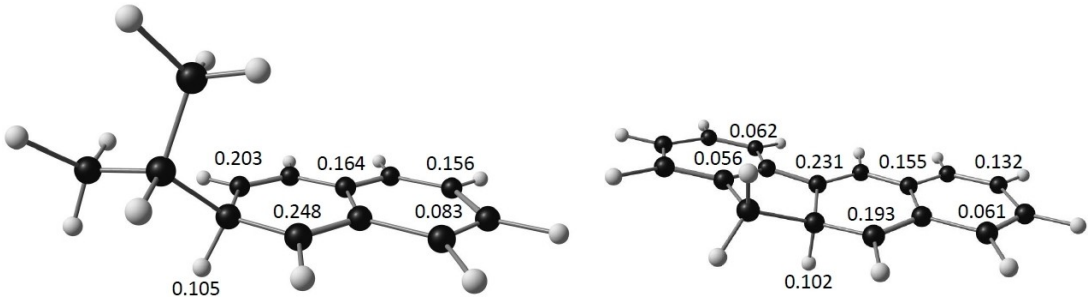

Figure 2. Charge distributions in *i*-Pr-naphthyl cation **22** (left) and benzyl-annelated naphthyl cation **18** (right).

examine the aromaticity of these rings (Figure 3). Compound **22** shows a higher aromatic character, supporting the contribution of the resonance structure shown in Figure 3. In the intermediate **18** the aromaticity is less pronounced, supporting the quinoidal structure.

The experimental study (Table 1) showed that even with substoichiometric amounts of amine the amine transfer product **21** is formed for the 1-indanone (**19**). Therefore, the rearrangement has been re-calculated for the aromatic 1-indanone (**19**) as well as the aliphatic 3-methylbutanal-derived dienophile. The elimination and the rearrangement seem to proceed *via* different pathways. In both cases the elimination is favored [for the indanone substrate with 15.1 kcal/mol *vs.* 19.3 kcal/mol starting from intermediate **16** and for the 3-methylbutanal with 16.6 kcal/mol (elimination) vs. 21.5 kcal/mol (rearrangement)]. Although the barrier for the elimination is computed to be lower than the rearrangement, protonation is essential for this pathway to occur. Even with substoichiometric amounts of amine, the quinodimethane intermediate is only present in comparable minor amounts. Hence, the protonation equilibrium should be on the amine side (Scheme 6, **16** *vs.* **17**). At lower concentrations of amine, however, this equilibrium will be shifted towards intermediate **17**, favoring the elimination, which is in accordance with the experimental data. Additionally, the eliminated product is thermodynamically preferred. Therefore, the elimination pathway is preferentially occurring at higher temperatures. This is again in agreement with the experiment and also supported by computing ΔG for this step at 110 °C compared to rt (see supporting information for details).

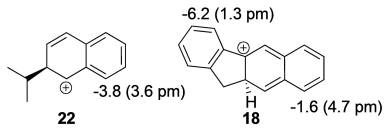

Figure 3. Most abundant resonance structures of *i*-Pr-naphthyl cation **22** (left) and annelated naphthyl cation **18** (right) with NICS(0) on examined rings and BLA in brackets.

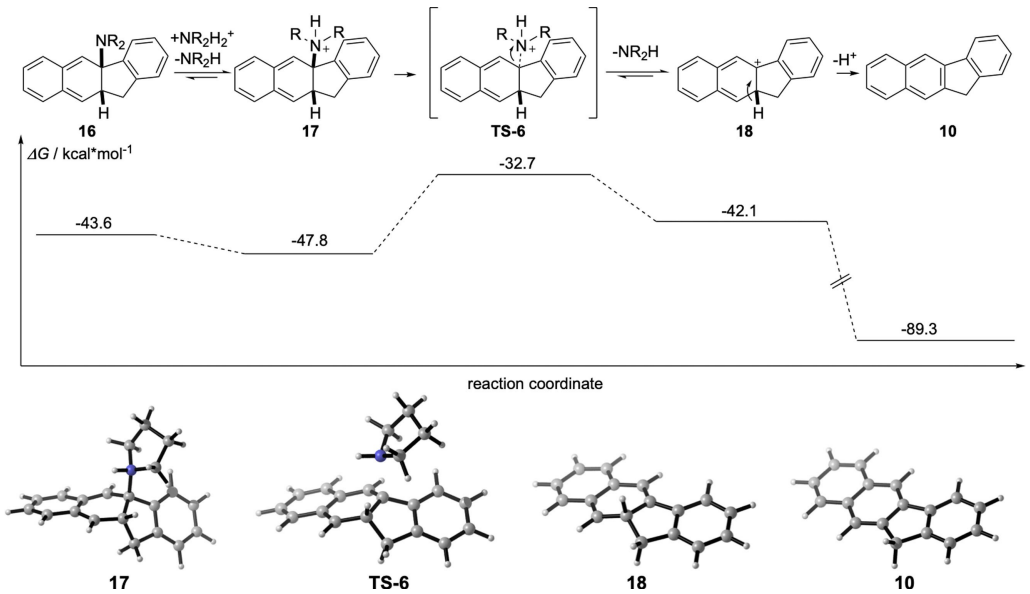

Scheme 6. Pathway from the quinodimethane intermediate **16** to the eliminated product **10** *via* an E1-type mechanism.

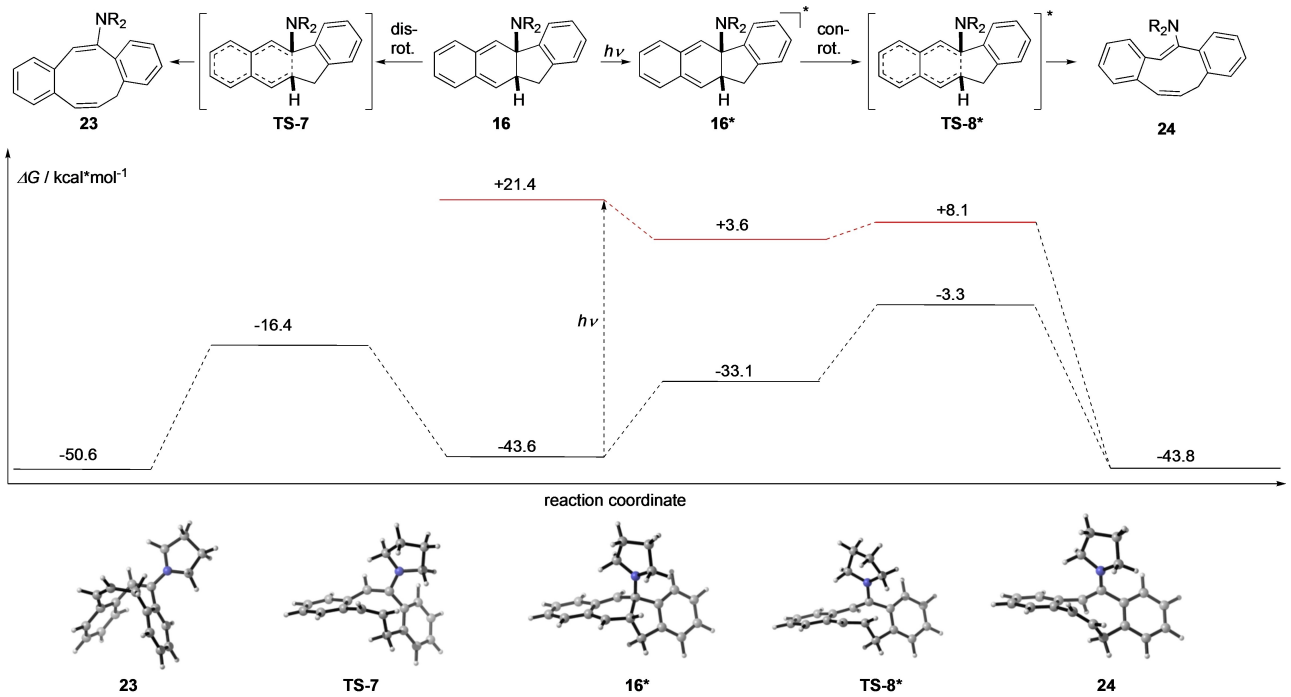

Scheme 7. Evaluation of the thermal and photo-induced ring opening of the quinodimethane intermediate **16** (black lines = ground state, red lines = excited states).

The third pathway is the PIRO reaction of the quinodimethane intermediate **16** (Scheme 7). According to the Woodward-Hoffmann rules, this 6π-electrocyclization has to progress thermally in a disrotatory fashion, and conrotatory under photochemical conditions. In principle, both pathways could be distinguished by the relative configuration of the two double bonds generated (**23** *vs.* **24**). However, the enamine can isomerize under the reaction conditions. As expected, mixtures of *E*- and *Z*-geometry have been observed.

First, a potential thermal mechanism has been computed. Such a process would require an activation energy of 27.2 kcal/mol, which would be much higher than any of the investigated elimination or rearrangement steps. TD-DFT computations project an intense absorption band at around 440 nm (65.0 kcal/mol) for the quinodimethane intermediate **16**, which is in good correlation with the applied wavelength between 400 and 500 nm. After excitation to the *S*1 state, thermal relaxation leads to structure **16***. From there, the ring-opened product can be accessed nearly barrierless (4.5 kcal/mol). Following relaxation to the *S*0 ground state provides the observed IEDDA/PIRO product. The final product absorbs at a much lower wavelength (390 nm), inhibiting a photochemical back reaction under the applied conditions. Hydrolysis of **24** sets free another 8.8 kcal/mol, giving finally access to product **8**.

Conclusion

The complete mechanism for all possible pathways of the domino processes initiated by the bidentate Lewis acid catalyzed IEDDA reaction of diazenes has been computationally evaluated. The initial IEDDA step with the enamine dienophile proceeds *via* a non-concerted process. The following N_2-extrusion occurs then after release of the catalyst to form the quinodimethane key intermediate. The elimination as well as the amine transfer reaction are very close in energy, although they proceed *via* different mechanisms: While for the elimination an E1-type pathway has been shown to be most feasible, the amine transfer operates along the already published bimolecular "enforced" concerted pathway.[9] Also, the photochemical ring opening has been computed proceeding by an excitation to the first excited state, from which the electrocyclization advances nearly barrierless to the final product. These results provide detailed information about the bidentate Lewis acid catalyzed domino IEDDA reaction, which will serve as a basis to develop new reactions and design novel catalysts in the future.

Experimental Section

Computations: Geometry optimizations, TD-DFT and IRC computations were conducted with the Gaussian 16 software package.[21] The opt = tight and int = ultrafine keywords were applied. Every optimized geometry was checked for the absence of imaginary frequencies in ground state and the presence of one imaginary frequency for transition states. All optimizations and frequency calculations were conducted for 298 K unless otherwise stated. For the time-dependent DFT computations also the previously optimized PBE0-D3BJ structures were used as input for further calculations.[22] In this way, excitation energies, as well as geometries of excited states were obtained. All T1-diagnostic values for

the high accuracy DLPNO-CCSD(T)/def2-TZVP single point energy computations were below 0.02 (maximum found T1 = 0.012825836).[23] Molecular structures were visualized using the CYLview software.[24]

Non-covalent Interaction Analysis (NCI): With the NCIPLOT 4.0 software[25] identification of non-covalent interactions from the reduced density gradient (s) is possible. This method is based on the electron density ρ and its derivatives. In this way, regions in the molecules are depicted as isosurfaces, indicating the locations of these interactions. They can be differentiated by taking into account the sign of the second density Hessian eigenvalue (λ_2). The colour code is further used to distinguish between attractive (blue), repulsive (red) and weak interactions (green). The following parameters on sign(λ_2)ρ were set: -2.0 (blue) < 0.0 (green) $<$ 2.0 (red). The final visualization of the respective molecules and isosurfaces was created with the VMD[26] software package.

General Information: Chemicals were purchased from Sigma-Aldrich, Acros Organics, Alfa Aesar, chemPUR, abcr GmbH or TCI Europe. Anhydrous solvents were purchased from Acros Organics. Deuterated solvents were purchased from Euriso-Top GmbH. Solids were dried over Sicapent® and under high vacuum if necessary. Technical grade solvents, used during work-up and purification, were distilled prior to use. Bidentate Lewis acid **3** was synthesized as described in literature[7b,27] and was stored in a nitrogen filled glove box. Sensitive reactions were performed in dry glassware under nitrogen-atmosphere using Schlenk-techniques or in a nitrogen-filled MBRAUN UNIlab glove box. Proton-Nuclear Magnetic Resonance (^{1}H NMR) spectra were measured on a Bruker Avance 400 (400 MHz) or Bruker Avance 600 (600 MHz). All measurements were performed at rt. Chemical shifts (δ) are reported in parts per million (ppm) relative to residual solvent signals or tetramethylsilane (TMS). Carbon-Nuclear Magnetic Resonance (^{13}C NMR) spectra were measured on a Bruker Avance 400 (101 MHz) or Bruker Avance 600 (151 MHz). All measurements were performed at rt. Chemical shifts (δ) are reported in parts per million (ppm) relative to residual solvent signals or tetramethylsilane (TMS). Mass spectra (MS) were recorded on a Bruker microTOF LC with an Electrospray-ionization source (ESI). Samples were dissolved in methanol. In positive ion detection mode, the capillary current was set to 4500 V with the end plate offset of -500 V. For column chromatography, Silica gel 60 (0.04–0.063 mm) from Macherey-Nagel GmbH & Co. was used. For thin layer chromatography (TLC), SIL G/UV254 with 0.2 mm SiO_2-layer thickness from Macherey-Nagel GmbH & Co. was used. Spots were detected with an UV-lamp at 254 or 366 nm wavelength.

Synthesis of the eliminated product 10 **and amine** 21: The reaction was set up in a nitrogen filled glovebox. Phthalazine (**1**) (13.3 mg, 100 μmol, 1.00 equiv.), 1-indanone (**19**) (13.6 mg, 100 μmol, 1.00 equiv.) and **3** (1.0 mg, 5.0 μmol, 5.0 mol%) were dissolved in dry dioxane (1.0 mL). Pyrrolidine was added to the reaction mixture. Afterwards, the reaction vessel was sealed and the reaction was performed under Schlenk conditions in the fume hood. The reaction mixture was heated to 110 °C in a sand bath. After one to four days, the reaction mixture was concentrated under reduced pressure. A green oil was obtained, which was purified by column chromatography (SiO_2: 7.0 g; eluent: toluene (100 mL) then toluene + 1% NEt_3 (~200 mL)) providing the eliminated product **10** as colorless solid and obtaining the not pure amine **21** as dark yellow oil. The amine **21** was purified by column chromatography (SiO_2: 5.0 g; eluent: cyclohexane/ethyl acetate + 1 % NEt_3 − 60/1) a second time to provide amine **21** as colorless oil. Elimination product **10**: ^{1}H NMR (400 MHz, $CDCl_3$ with 0.03% v/v TMS): δ/ppm = 8.21 (s, 1H), 8.01–7.82 (m, 4H), 7.61–7.53 (m, 1H), 7.52–7.33 (m, 4H), 4.10 (s, 2H). The analytical data corresponds to the literature.[28] Rearrangement product **21**: ^{1}H NMR (600 MHz, $CDCl_3$ with 0.03% v/v TMS): δ/ppm = 7.69–7.64 (m, 1H), 7.62 (dd, J = 6.2, 2.3 Hz, 1H), 7.35 (dd, J = 6.2, 2.2 Hz, 1H), 7.30–7.19 (m, 5H), 6.84 (d, J = 3.0 Hz, 1H), 4.18 (d, J = 14.7 Hz, 1H), 3.34 (dd, J = 15.6, 8.1 Hz, 1H), 3.18 (dtd, J = 15.2, 7.9, 3.0 Hz, 1H), 3.05 (dq, J = 8.1, 4.4 Hz, 2H), 2.92 (dt, J = 15.8,7.9 Hz, 3H), 1.95–1.86 (m, 4H). ^{13}C NMR (151 MHz, $CDCl_3$ with 0.03% v/v TMS): δ/ppm = 146.8, 146.6, 139.5, 137.9, 136.1, 128.5, 126.9, 126.8, 126.0, 125.3, 120.9, 115.7, 63.0, 48.1, 40.6, 38.2 (2 C), 31.1, 27.2, 24.4 (2 C). HRMS (ESI) m/z: $[M+H]^+$ Calc. for $C_{21}H_{22}N^+ = 288.1747$; found: 288.1744.

Acknowledgements

The authors thank the DFG for funding and Heike Hausmann (Institute of Organic Chemistry, Justus Liebig University, Giessen) for NMR-measurements. Open access funding enabled and organized by Projekt DEAL.

Conflict of Interest

The authors declare no conflict of interest.

Keywords: Cycloaddition · Density functional theory · Elimination · Organocatalysis · Photochemistry

[1] a) K. C. Nicolaou, T. Montagnon, G. Vassilikogiannakis, *Angew. Chem. Int. Ed.* **2002**, *41*, 1668–1698; *Angew. Chem.* **2002**, *114*, 1742–1773; b) J. A. Funel, S. Abele, *Angew. Chem. Int. Ed.* **2013**, *52*, 3822–3863; *Angew. Chem.* **2013**, *125*, 3912–3955; c) N. Zydziak, B. Yameen, C. Barner-Kowollik, *Polym. Chem.* **2013**, *4*, 4072–4086.
[2] a) A. C. Knall, C. Slugovc, *Chem. Soc. Rev.* **2013**, *42*, 5131–5142; b) Z. M. Png, H. Zeng, Q. Ye, J. Xu, *Chem. Asian J.* **2017**, *12*, 2142–2159; c) J. Zhang, V. Shukla, D. L. Boger, *J. Org. Chem.* **2019**, *84*, 9397–9445; d) E. Brachet, P. Belmont, *Curr. Org. Chem.* **2016**, *20*, 2136–2160.
[3] For selected applications of IEDDA reaction of diazenes in total synthesis, see: a) J. L. Graham, J. Bodwell, *Angew. Chem. Int. Ed.* **2002**, *41*, 3261–3262; *Angew. Chem.* **2002**, *114*, 3395–3396; b) S. Yang, K. Sankar, C. K. Skepper, T. J. Barker, J. C. Lukesh 3rd, D. M. Brody, M. M. Brutsch, D. L. Boger, *Chem. Sci.* **2017**, *8*, 1560–1569; c) M. L. Landry, G. M. McKenna, N. Z. Burns, *J. Am. Chem. Soc.* **2019**, *141*, 2867–2871.
[4] a) B. L. Oliveira, Z. Guo, G. J. L. Bernardes, *Chem. Soc. Rev.* **2017**, *46*, 4895–4950; b) Y. Li, H. Fu, *ChemistryOpen* **2020**, *9*, 835–853; c) D. Ganz, D. Harijan, H.-A. Wagenknecht, *RSC Chem. Biol.* **2020**, *1*, 86–97; d) C. G. Parker, M. R. Pratt, *Cell* **2020**, *180*, 605–632; e) Y. Wang, C. Zhang, H. Wu, P. Feng, *Molecules* **2020**, *25*, 5640; f) E. Kim, H. Koo, *Chem. Sci.* **2019**, *10*, 7835–7851.
[5] G. Xu, X. Bai, Q. Dang, *Acc. Chem. Res.* **2020**, *53*, 773–781.
[6] a) Y. F. Yang, Y. Liang, F. Liu, K. N. Houk, *J. Am. Chem. Soc.* **2016**, *138*, 1660–1667; b) K. Lang, S. Mayer, *Synthesis* **2016**, *49*, 830–848; c) S. D. Schnell, M. Schilling, J. Sklyaruk, A. Linden, S. Luber, K. Gademann, *Org. Lett.* **2021**, *23*, 2426–2430.
[7] a) S. N. Kessler, H. A. Wegner, *Org. Lett.* **2010**, *12*, 4062–4065; b) S. N. Kessler, M. Neuburger, H. A. Wegner, *Eur. J. Org. Chem.* **2011**, 3238–3245; c) L. Schweighauser, I. Bodoky, S. N. Kessler, D. Haussinger, C. Donsbach, H. A. Wegner, *Org. Lett.* **2016**, *18*, 1330–1333.
[8] B. Yang, S. Gao, *Chem. Soc. Rev.* **2018**, *47*, 7926–7953.
[9] S. Ahles, S. Götz, L. Schweighauser, M. Brodsky, S. N. Kessler, A. H. Heindl, H. A. Wegner, *Org. Lett.* **2018**, *20*, 7034–7038.
[10] S. Ahles, J. Ruhl, M. A. Strauss, H. A. Wegner, *Org. Lett.* **2019**, *21*, 3927–3930.
[11] J. Ruhl, S. Ahles, M. A. Strauss, C. M. Leonhardt, H. A. Wegner, *Org. Lett.* **2021**, *23*, 2089–2093.
[12] C. Adamo, V. Barone, *J. Chem. Phys.* **1999**, *110*, 6158–6170.
[13] F. Weigend, R. Ahlrichs, *Phys. Chem. Chem. Phys.* **2005**, *7*, 3297–3305.

[14] a) S. Grimme, S. Ehrlich, L. Goerigk, *J. Comput. Chem.* **2011**, *32*, 1456–1465; b) S. Grimme, J. Antony, S. Ehrlich, H. Krieg, *J. Chem. Phys.* **2010**, *132*, 154104.
[15] A. V. Marenich, C. J. Cramer, D. G. Truhlar, *J. Chem. Phys. B* **2009**, *113*, 6378–6396.
[16] C. Riplinger, B. Sandhoefer, A. Hansen, F. Neese, *J. Chem. Phys.* **2013**, *139*, 134101.
[17] a) F. Neese, *WIREs Comput. Mol. Sci.* **2011**, *2*, 73–78; b) F. Neese, *WIREs Comput. Mol. Sci.* **2017**, *8*, 33.
[18] Y. F. Yang, P. Yu, K. N. Houk, *J. Am. Chem. Soc.* **2017**, *139*, 18213–18221.
[19] S. N. Kessler, M. Neuburger, H. A. Wegner, *J. Am. Chem. Soc.* **2012**, *134*, 17885–17888.
[20] J. Contreras-García, E. R. Johnson, S. Keinan, R. Chaudret, J.-P. Piquemal, D. N. Beratan, W. Yang, *J. Chem. Theory Comput.* **2011**, *7*, 625–632.
[21] M. J. Frisch, G. W. Trucks, H. B. Schlegel, G. E. Scuseria, M. A. Robb, J. R. Cheeseman, G. Scalmani, V. Barone, G. A. Petersson, H. Nakatsuji, X. Li, M. Caricato, A. V. Marenich, J. Bloino, B. G. Janesko, R. Gomperts, B. Mennucci, H. P. Hratchian, J. V. Ortiz, A. F. Izmaylov, J. L. Sonnenberg, Williams, F. Ding, F. Lipparini, F. Egidi, J. Goings, B. Peng, A. Petrone, T. Henderson, D. Ranasinghe, V. G. Zakrzewski, J. Gao, N. Rega, G. Zheng, W. Liang, M. Hada, M. Ehara, K. Toyota, R. Fukuda, J. Hasegawa, M. Ishida, T. Nakajima, Y. Honda, O. Kitao, H. Nakai, T. Vreven, K. Throssell, J. A. Montgomery Jr., J. E. Peralta, F. Ogliaro, M. J. Bearpark, J. J. Heyd, E. N. Brothers, K. N. Kudin, V. N. Staroverov, T. A. Keith, R. Kobayashi, J. Normand, K. Raghavachari, A. P. Rendell, J. C. Burant, S. S. Iyengar, J. Tomasi, M. Cossi, J. M. Millam, M. Klene, C. Adamo, R. Cammi, J. W. Ochterski, R. L. Martin, K. Morokuma, O. Farkas, J. B. Foresman, D. J. Fox, Wallingford, CT, **2016**.
[22] a) C. Adamo, D. Jacquemin, *Chem. Soc. Rev.* **2013**, *42*, 845–856; b) E. Runge, E. K. U. Gross, *Phys. Rev. Lett.* **1984**, *52*, 997–1000.
[23] T. J. Lee, P. R. Taylor, *Int. J. Quantum Chem.* **1989**, *36*, 199–207.
[24] C. Y. Legault, Université de Sherbrooke, Quebec, Canada, **2009**, http://www.cylview.org.
[25] E. R. Johnson, S. Keinan, P. Mori-Sánchez, J. Contreras-García, A. J. Cohen, W. Yang, *J. Am. Chem. Soc.* **2010**, *132*, 6498–6506.
[26] W. Humphrey, A. Dalke, K. Schulten, *J. Mol. Graphics* **1996**, *14*, 33–38.
[27] L. Hong, S. Ahles, A. H. Heindl, G. Tietcha, A. Petrov, Z. Lu, C. Logemann, H. A. Wegner, *Beilstein J. Org. Chem.* **2018**, *14*, 618–625
[28] M. P. C. B. Rao, H. Ila, H. Junjappa, *Tetrahedron* **1991**, *47*, 3499–3510.

Manuscript received: April 20, 2021
Revised manuscript received: May 26, 2021
Accepted manuscript online: May 28, 2021